

## Efficiently and Conveniently Heparin/ PEG-PCL Core-Shell Microcarriers Fabrication and Optimization via Coaxial-Electrospraying

Ying Mao<sup>1</sup>, Chaojing Li<sup>1</sup>, Peng Ge<sup>1</sup>, Fujun Wang<sup>1,\*</sup> and Lu Wang<sup>1,\*</sup>

**Abstract:** Heparin/ PEG-PCL core-shell microcarriers were fabricated in one-step via coaxial-electrospraying technology. Optimization of the coaxial-electrospraying processing is by controlling the PEG-PCL concentration, applied voltage, receiving distance, and feed rate. The influence of the electro spray parameters on microsphere morphology was studied by optical microscopy and scanning electron microscopy. The functional groups and components of the electro sprayed microspheres were characterized by Fourier transform infrared spectroscopy (FTIR). Transmission electron microscope (TEM) observation proved the core-shell structure of heparin-loaded PEG-PCL microspheres. Drug loading and releasing study demonstrated that PEG-PCL concentration could control the encapsulation efficiency and releasing activity of the heparin in the microspheres. The hemocompatibility assays indicated that the anticoagulant property of PCL membranes improved markedly, when the surface modified with heparin-loaded PEG-PCL microspheres.

**Keywords:** Heparin-loaded microspheres, core-shell structure, coaxial-electrospraying, sustained-release, anticoagulation.

### 1 Introduction

As one of the most efficient and promising anticoagulants, heparin has been incorporated into biomedical devices through various methods. Heparinized techniques have been recognized as successful strategies to prevent thrombus formation and to improve the blood compatibility of biomaterials or devices [Heyligers, Verhagen, Rotmans et al. (2006); Hoshi, Van Lith, Jen et al. (2013); Maitz, Zitzmann, Hanke et al. (2017)]. In the past decades, many heparinized techniques have been reported, typically including physical adsorption, covalent immobilization, and layer-by-layer self-assembly [Murugesan, Xie and Linhardt (2008); Li, Xie, Pan et al. (2014); Bao, Wu, Sun et al. (2015)]. Physical adsorption is the most convenient method to achieve material heparinized, but the amount of heparin immobilized on the surface of the materials is limited, and heparin is easily replaced by other anion substances in the blood. Heparin could be tightly immobilized on biomaterials or devices through the covalently bonded method. While the native conformation of heparin would be damaged, thus the anticoagulant effect of heparin

---

<sup>1</sup> Key Laboratory of Textile Technology, Ministry of Education, College of textiles, Donghua University, Songjiang District, Shanghai, 201620, China.

\* Corresponding Author: Fujun Wang. E-mail: wfj@dhu.edu.cn;

Lu Wang. E-mail: wanglu@dhu.edu.cn.

would be decreased [Biran and Pond (2017)]. For layer-by-layer self-assembly method, the combination of heparin and materials is not stable enough to withstand long-term exposure *in vivo* [Yang, Wang, Luo et al. (2010)].

With the development of the polymeric drug delivery system, many researchers pay more attention to fabricate the heparin-functionalized microcarriers including heparin-loaded micelles [Lee, Bae, Joung et al. (2008); Zhao, Lord and Stenzel (2013); Mei, Liu, Zhang et al. (2016)] and micro/nanospheres [Tong, Chen, Chen et al. (2013); Han, Zhou, Yang et al. (2015); Mouftah, Abdel-Mottaleb and Lamprecht (2016); Lamprecht, Ubrich and Maincent (2007)]. Those structures exhibit several unique features, such as improved the bioavailability of heparin, reduced systemic side effects, controlled drug release rate and avoided dosage limitation. The heparin-loaded microencapsulation techniques include emulsification [Han, Zhou, Yang et al. (2015); Mouftah, Abdel-Mottaleb and Lamprecht (2016)], complex coacervation [Mouftah, Abdel-Mottaleb and Lamprecht (2016); Tsung and Burgess (1997)], and self-assembly [Mei, Liu and Zhang (2016), Qi, Sun and Jing (2012)]. Among the encapsulation methods, the limitations of emulsification method are broad particle size distribution and low encapsulation efficiency. Although complex coacervation shows high encapsulation efficiency, it can result in hematotoxicity due to the addition of undesirable toxic residues. In contrast, self-assembly technique is relatively versatile and controllable, but time and material wastage limit this approach.

Nowadays, coaxial electrospraying is of great scientific interest as an emerging method to fabricate drug-loaded microcarriers of the core-shell structure, which shows many advantages over other traditional methods in terms of devices, operation and material limit, etc. Many scholars conducted a series of research to fabricate core-shell microspheres via coaxial electrospraying [Hwang, Jeong and Cho (2008); Cao, Wang, Tu et al. (2014); Zamani, Prabhakaran, Thian et al. (2014); Wang, Wei, Zhang et al. (2015); Gao, Zhao, Chang et al. (2016)]. Hwang Y et al. [Hwang, Jeong and Cho (2008)] produced uniform-sized microcapsules consisting of polystyrene or polymethylmethacrylate core and poly( $\epsilon$ -caprolactone) shell by utilizing the coaxial electrospraying. Rasekh et al. [Rasekh, Young, Roldo et al. (2015)] described the preparation of core-shell peptide encapsulated nanostructure via electrospraying technique. Gao et al. [Gao, Zhao, Chang et al. (2016)] optimized the shell thickness-to-radius ratio for fabricating the oil-encapsulated polymeric microspheres. However, there is seldom research on fabricating heparin-loaded microspheres via coaxial-electrospraying [Li, Wang, Ge et al. (2017)].

In this study, the main objective was to fabricate the heparin-loaded microspheres with core-shell structure via coaxial-electrospraying. The microsphere size and morphology under different experimental parameters were characterized. And the anticoagulant properties, heparin loading and release activities of the core-shell microspheres were also investigated.

## **2 Experimental**

### **2.1 Materials**

Heparin and Toluidine blue O (TBO) were obtained from Sinopharm Chemical Reagent Co., Ltd. (Shanghai, China). Poly (ethylene glycol)-polycaprolactone with the ethylene glycol-caprolactone molar ratio of 1:2 (PEG-PCL, Mw: 15 kDa) was supplied by Jinan

Daigang Biomaterial Co., Ltd. (Shandong, China). Dichloromethane (DCM) was purchased from Shanghai Lingfeng Chemical Reagent Co., Ltd. (Shanghai, China) and used as solvent directly. Phosphate-buffered saline (PBS) was purchased from Solarbio (Shanghai, China). All chemical reagents were used as received without any further purification.

### ***2.2 Preparation of electrospraying solutions***

PEG-PCL was dissolved in DCM and stirred for 2 h to obtain homogeneous solutions, with concentration of 2%, 4% and 6% (w/v), respectively. Simultaneously, heparin powder was dissolved in deionized water at a drug concentration of 0.5% (w/v). All of the solutions were then used immediately for electrospray.

### ***2.3 Preparation of the pure and drug-load microspheres***

Two 5 mL syringes containing heparin and PEG-PCL solution, respectively, were connected to the coaxial nozzle, consisting of an inner needle (inner diameter (ID): 0.50 mm; outer diameter (OD): 0.90 mm) and an outer needle (ID: 1.40 mm; OD: 1.90 mm). All of electrospray processes were carried out at 25 °C, and the feed rate ratio of inner and outer solutions was 1:6. The outer solution flow rate was 0.25-1.25 mL/h, the applied voltage and the distance between the spinneret and the collector were maintained at 6-12 kV and 10-25 cm, respectively. The grounded aluminum plate with a piece of fixed glass plate or PCL membrane was placed to collect pure or drug-load microspheres. The resulting samples were dried and stored in plastic bags in a desiccator until used.

### ***2.4 Morphology of microspheres***

Morphologies of the pure microspheres collected on glass plate were investigated with a light compound SMZ745T microscopy (optical microscopy, OM, Nikon Imaging Sales Co. Ltd., Shanghai, China). The surface morphologies of drug-loaded microspheres were analyzed by scanning electron microscopy (SEM; Hitachi, TM-3000, Japan), and the samples were sputter-coated with gold for better conductivity during imaging. The average diameters and particle size distribution of microspheres were calculated using Adobe Acrobat Pro software. At least 100 random measurements from several images were used to obtain the mean values.

### ***2.5 Structure analysis***

The chemical characteristics of the samples were examined in KBr pellets by FTIR spectroscopy (Nicolet 6700, Thermo Fisher Scientific Inc. MA, USA). The samples were scanned against an air background at wave numbers ranging from 4000  $\text{cm}^{-1}$  to 400  $\text{cm}^{-1}$ . Measurements were performed on heparin powder, pure and heparin-loaded microspheres. The core-shell structure of heparin-loaded microspheres was investigated by TEM (JEM-2100F, JEOL Ltd., Tokyo, Japan).

### ***2.6 Drug loading and release study***

The quantity of drug loaded in the core-shell microspheres was determined by UV-visible spectrophotometer (Patten TU-1901, Beijing Purkinje General Instrument Co., Ltd, Beijing, China). 100 mg microspheres were dissolved completely in 5 mL methylene

chloride (oil phase), 5 mL deionized water was then added and vibrated the mixture for 10 min to extract heparin from the oil phase. After 10 min' standing, the oil separates itself from water phase. The water phase was collected, and the absorbance was measured at 631 nm. The encapsulation efficiency (EE) of the heparin-loaded microspheres was calculated as follows:

$$EE = \frac{\text{actual amount of heparin loaded in microspheres}}{\text{theoretical amount of heparin loaded in microspheres}} \times 100\%$$

The heparin release behavior of the core-shell microspheres was measured by the immersion of a known mass of material (30 mg) in 8 ml of PBS (PH=7.4) in centrifuge tubes, which were shaken in an incubator for 15 days at 37°C. At procedural time points, 2 mL solution was taken out and an equal amount of the fresh buffer solution was supplemented. To evaluate the accumulative release of heparin, 3 mL TBO was added into 2 mL of the release medium collected at different time points. After incubation at 37°C for 30 min, the heparin/TBO precipitate was centrifuged and the absorbance at 631 nm was measured after the water phase was collected.

### **2.7 Hemocompatibility**

Fresh rabbit blood was centrifuged (5000 rpm, 5 min) and washed 5 times with PBS to remove the serum. Erythrocytes were diluted 35 times with PBS to obtain human red bleed cells (HRBCs). Then, 1×1 cm<sup>2</sup> samples (PCL membranes modified or unmodified by drug-loaded microspheres) were immersed in 1 mL HRBCs and 4 mL PBS. The Eppendorf tubes were incubated at 37°C for 2 h and then centrifuged at 5000 rpm for 5 min. Absorbance at 540 nm (D<sub>t</sub>) of the supernatant was determined using a microplate reader (Multiskan FC, Thermo). In this assay, HRBCs were treated with 4 mL distilled water or PBS buffer as positive control or negative control, their absorptions (D<sub>pc</sub> and D<sub>nc</sub>) were also measured. The hemolysis percentage was calculated as (D<sub>t</sub>-D<sub>nc</sub>/D<sub>pc</sub>-D<sub>nc</sub>)×100%. The hemolysis data were expressed as the mean of three replicates.

The anticoagulant properties were evaluated by modified re-calcified plasma and whole blood clotting method [Li, Wang and Ge (2017)], 20 μL fresh rabbit blood and 10 μL of 0.2 M CaCl<sub>2</sub> solution were successively dropped onto 1×1 cm<sup>2</sup> samples, followed by incubation at 37°C for a certain time. Then 5 mL deionized water was added and followed to be incubated 5 min. The absorbance of the resulting hemoglobin solution was measured at 540 nm.

### **2.8 Statistical analysis.**

The statistical analysis were performed using IBM SPSS Statistics 23 with significant level  $p < 0.05$ . The data reported were the means and standard deviations, and the error bars in the figures correspond to one standard deviation. The data in the figures were marked by (\*) for  $p < 0.05$  and (\*\*\*) for  $p < 0.001$ .

### **3 Results and discussion**

#### ***3.1 Effect of electrospaying variables on microspheres diameter***

The effects of electrospay parameters including of polymer concentration, applied voltage, flow rate and received distance of pure microspheres were analyzed (Fig. 1). As shown in Fig. 1(a), Polymer concentration played an important role in the morphology of electrospayed microsphere. For a concentration of the PEG-PCL solution lower than 2%, the monodispersity of microspheres was ideal, but the morphology was irregular. This is attributed to the viscosity of electrospaying solution too low to form uniform microspheres. With the increasing of PEG-PCL concentration, the morphology of the PEG-PCL microspheres gradually changed from a sphere to a spinning shape, due to the surface tension less than the viscous force of the solution for a concentration higher than 6%.

The effect of applied voltage on microspheres diameter is shown in Fig. 1(b). As the applied voltage enhanced, the microsphere size became smaller. It was mainly because of the higher electrostatic force of polymer with the enhancement of the applied voltage, leading to better fabrication of atomization droplet, smaller average diameter of the droplet, and smaller size of the obtained microspheres. In addition, when the applied voltage was above 12 kV, jet flow began to go unsteady. It results from the attraction force between negative electrode and polymer increased, when the applied voltage enhanced. Then, the stability of the Taylor cone forming at nozzle was destroyed and multi-stage injection was formed. The results indicated that the most suitable applied voltage was 10 kV.

Morphology, size, and distribution of microspheres under different receiving distance were observed in Fig. 1(c). When receiving distance increased, the average diameter firstly decreased and then increased. It was because that the distance of solvent evaporating from jet fluid was longer, and the quantity of volatile solvent increased meanwhile electric field intensity weakened, which results in the average diameter of microspheres enlarged. Besides, the obtained microspheres were spindle or clubbed shape, and the particle size distribution was not uniform. The results showed the reasonable receiving distance was 15 cm.

The effect of feed rate on microspheres diameter could not be ignored as well. As shown in Fig. 1(d), the average diameter of microspheres increased as the feed rate rose. It was attributed to the increase of extrusive polymer amount per unit time with the increase of feed rate. And the optimizing feed rate was 0.5 mL/h.

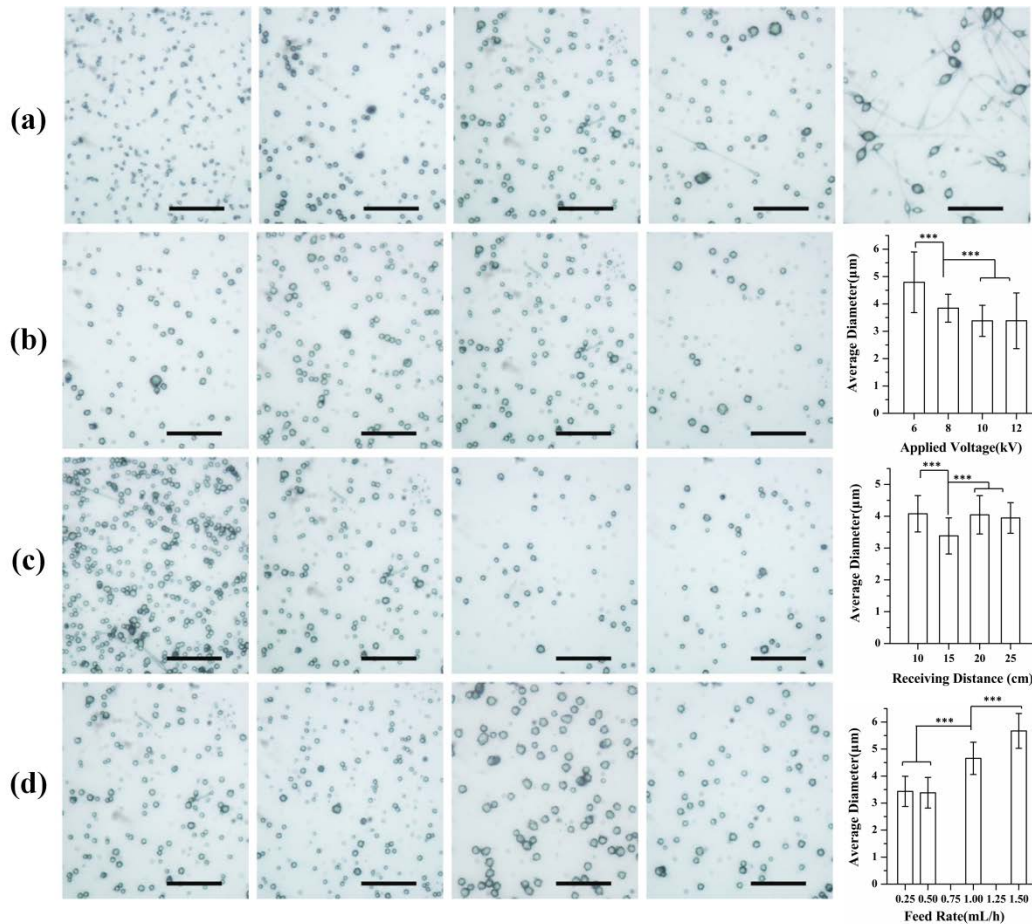


**Figure 1:** OM images and diameters distribution histograms of pure microspheres under different experiment parameter (a) PEG-PCL concentration (1%, 2%, 4%, 6% and 8%), (b) Applied voltage (6 kV, 8 kV, 10 kV and 12 kV), (c) Receiving distance (10 cm, 15 cm, 20 cm and 25 cm), (d) Feed rate (0.25 mL/h, 0.5 mL/h, 1.0 mL/h and 1.5 mL/h). Scale bar=35 μm. Significant difference are marked by (\*\*\*) for  $p < 0.001$

### 3.2 Morphology of heparin-loaded microspheres

Microscopic evaluation showed that the average diameter of heparin-loaded microspheres fabricated by 2%, 4% and 6% (w/v) PEG-PCL solution (applied voltage=10 kV, receiving distance=15 cm, feed rate=0.5 mL/h) was similar to the pure microspheres (Fig. 2). And both of the diameter increased with the PEG-PCL concentration increased. However, the diameter of heparin-loaded microspheres ( $3.52 \pm 0.71 \mu\text{m}$ ) containing 4% (w/v) PEG-PCL is a little bigger than pure microspheres diameter ( $3.50 \pm 0.56 \mu\text{m}$ ). The results revealed that the morphology of core-shell microspheres was affected by shell polymer as well as core drug.

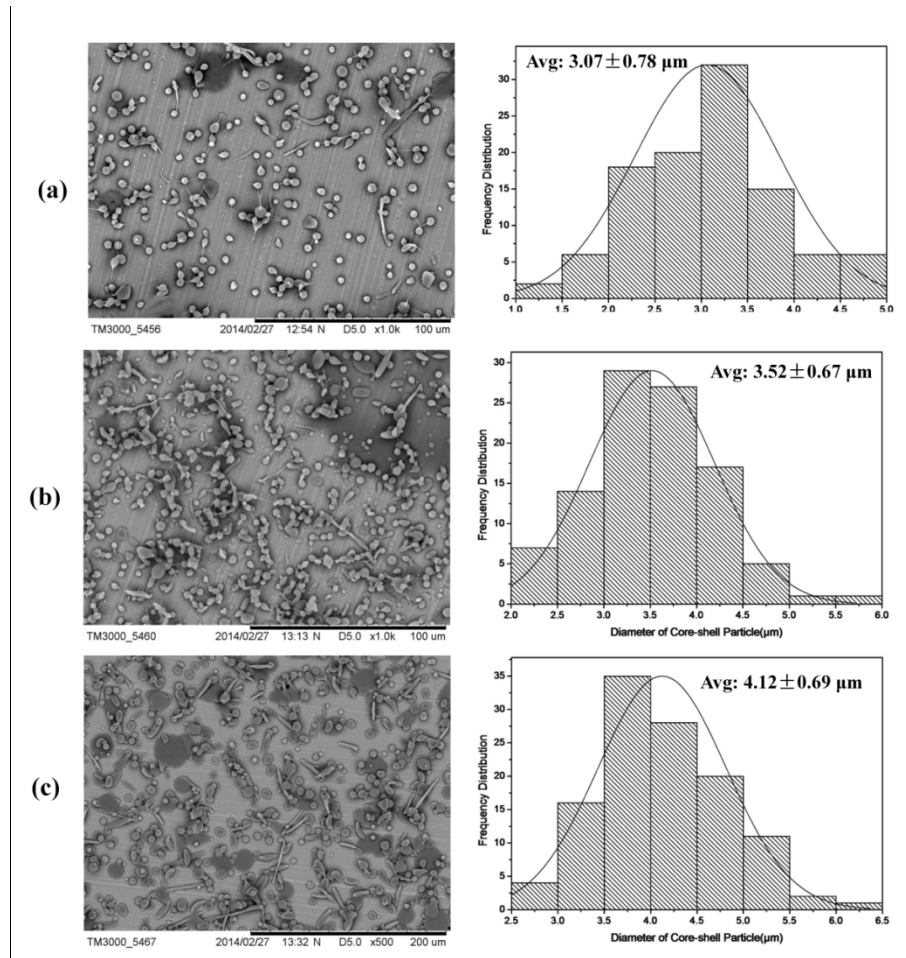


**Figure 2:** SEM images and diameter distribution histograms of heparin-loaded microspheres under different PEG-PCL concentration: (a) 2 wt. %, (b) 4 wt. % and (c) 6 wt. %

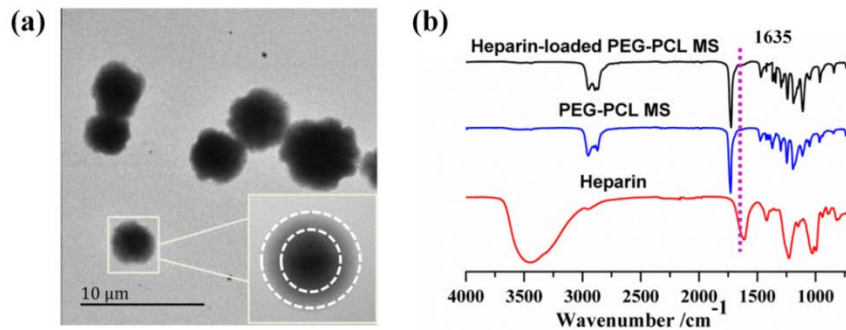


**Figure 3:** (a) TEM images of heparin-loaded microspheres, (b) FTIR spectra

### 3.3 Core-shell Structure of microspheres and drug release evaluation

It was obviously that the microspheres were core-shell structure in Fig. 3(a), where the core of the microsphere was darker than the shell part. FTIR spectrum showed in Fig. 3(b), the typical absorption peak at  $1635\text{ cm}^{-1}$  was due to  $\text{-C=O}$  stretching of  $\text{-CONH}_2$  group in heparin molecule appeared in heparin-loaded PEG-PCL MS FTIR spectrum, which demonstrated existence of heparin ingredient.

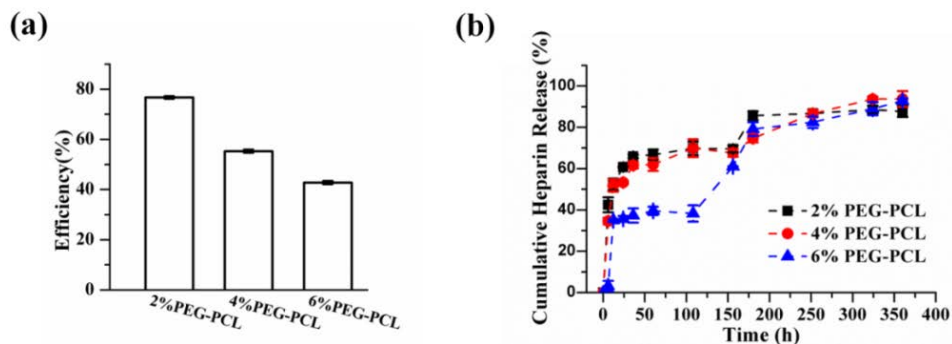


**Figure 4:** Quantification of heparin encapsulated in microspheres with different PEG-PCL concentration (a) Efficiency of encapsulated heparin in microspheres, (b) Cumulative heparin release profiles

As shown in Fig. 4(a), the encapsulation efficiency is orderly 76.7%, 55.3% and 42.8% for the drug-loaded microspheres with PEG-PCL concentration of 2%, 4% and 6% (w/v). The encapsulation efficiency tended to decrease with the increase of the PEG-PCL concentration, which resulted from the loss of heparin during the process of solvent evaporation. Due to evaporation of the solvent, the higher the solution concentration outer was, the lower encapsulation efficiency of shell polymer for similar microspheres was.

The heparin release activity from the drug-loaded microspheres was investigated over 330 h. The release profiles of heparin were shown in Fig. 4(b). The drug-loaded microspheres with different amounts of PEG-PCL showed similar release profile trend, especially for the microspheres with 2% and 4% PEG-PCL. Both of them exhibited an initial relatively fast release in the first several hours, and almost 50 h later, the release speed slowed down and went to steady along with the incubation time (350 h). The initial fast release was probably attributed to the diffusion of heparin near the surface of the microspheres, followed by the evaporation of the solvent. And the later slow release resulted from the seeping of heparin with the gradual degradation of PEG-PCL.

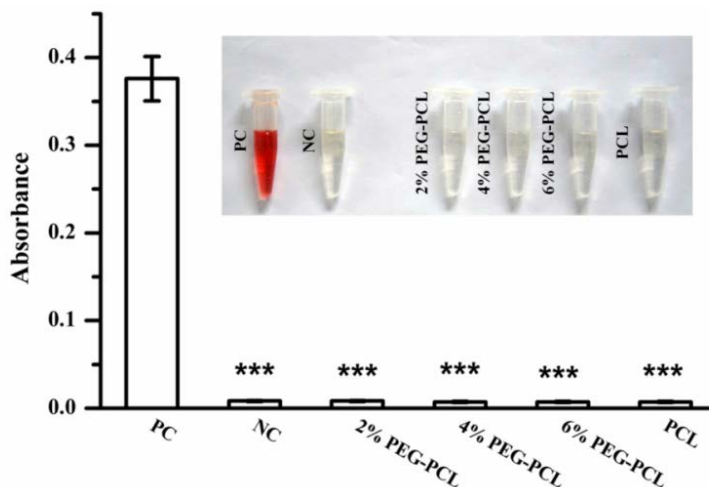


**Figure 5:** Mean hemolytic assays results. HRBCs exposed to PCL membranes and the modified PCL membranes with heparin-loaded microspheres (2%, 4% and 6% PEG-PCL) are compared with those exposed to water (positive control, PC) and PBS solution (negative control, NC). Mean data for each sample (n=3). Significant difference are marked by (\*\*\*) for  $p < 0.001$  compared with the positive control

### 3.4 Hemocompatibility

Hemolysis is a major concern for biomedical devices directly contacting with blood, and it's important and necessary to prevent hemolysis of biomaterials. The hemolytic activity of the samples is shown in Fig. 5. The absorbance of negative control is around 0.08, while all samples showed lower absorbance (below 0.08), whose degree of hemolysis was considered 0%. It is indicated that there was no significant hemolytic activity, similar to the negative control.

Anticoagulant property of samples was carried out by absorbance of the resulting hemoglobin solution shown in Fig. 6. The absorbance of PCL membranes with or without heparin-loaded microspheres maintained above 0.11 during the first 5 min, however, the silicon plate showed a significant absorbance decrease (below 0.08). As the time goes, the absorbance of all samples became lower. At 20 min, there is an obvious decrease of the PCL absorbance, lower than the absorbance of silicon plate. The phenomenon might be due to the hydrophobicity of PCL materials, the benefit to prevent adhesion of protein and red blood cell before PCL membranes were completely saturated. However, PCL membranes with heparin-loaded microspheres showed significantly higher absorbance (above 0.08) at 60 min. The result revealed that heparin-loaded microspheres modified PCL membranes showed better anticoagulant effectiveness.

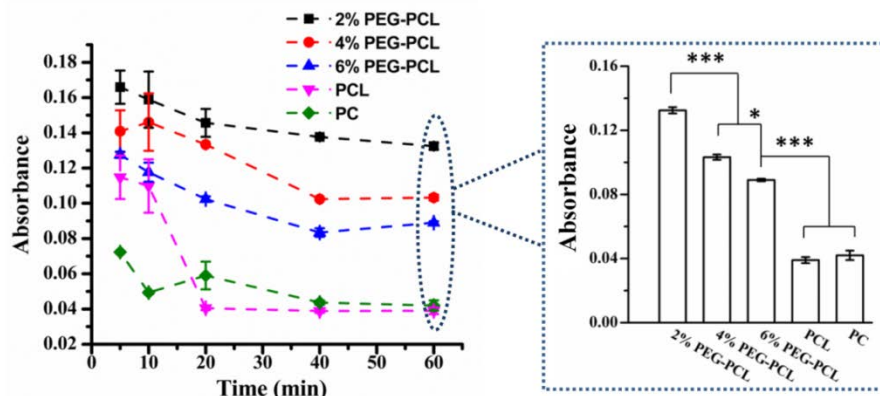


**Figure 6:** *In vitro* blood clotting test. Mean data for each sample (n=3). Significant difference are marked by (\*) for  $p < 0.05$  and (\*\*\*) for  $p < 0.001$

#### 4 Conclusions

The heparin-loaded microspheres with core-shell structure were successfully prepared via coaxial-electrospraying. OM images showed that the morphology, size, and distribution of microspheres could be controlled via adjusting the polymer concentration, applied voltage, receiving distance and flow rate. TEM images and FTIR spectrum demonstrated the core-shell structure of electrospayed microsphere. The results of heparin-release studies indicated that the core-shell microspheres exhibited an initial relatively fast release with the first 20 h, which would be helpful to prevent the blood coagulation immediately. The release speed slowed down and went to steady along with the incubation time (350 h) about 50 h later, which could be beneficial to a prolonged anticoagulant activity. As the results, the PCL membranes modified with heparin-loaded PEG-PCL microspheres had a continuous and effective anticoagulant property and no hemolysis. The entire results suggested that the electrospayed heparin-loaded microspheres with core-shell structure were of great potential for candidates used for the anticoagulant modification.

**Acknowledgement:** This work was financially supported by “111” project (B07024), the Fundamental Research Funds for the Central Universities, Science and Technology Support Program of Shanghai (Grant No. 16441903803), and National Postdoctoral Foundation (Grant No. 2016M590299).

#### References

- Bao, J.; Wu Q.; Sun, J.; Zhou, Y.; Wang, Y. et al.** (2015): Hemocompatibility improvement of perfusion-decellularized clinical-scale liver scaffold through heparin immobilization. *Scientific Reports*, vol. 5, pp. 10756-10768.
- Biran, R.; Pond, D.** (2017): Heparin coatings for improving blood compatibility of medical devices. *Advanced Drug Delivery Reviews*, vol. 112, pp. 12-23.

**Cao, L. H.; Wang, H. J.; Tu, K. H.; Jiang, H. L.; Wang, L. Q. et al.** (2014): Core-shell nanoparticles fabricated by tri-capillary coaxial electrospray and template removal method for protein delivery. *Acta Polymerica Sinica*, pp. 1238-1243.

**Gao, Y.; Zhao, D.; Chang, M. W.; Ahmad, Z.; Li, J. S. et al.** (2016): Optimising the shell thickness-to-radius ratio for the fabrication of oil-encapsulated polymeric microspheres. *Chemical Engineering Journal*, vol. 284, pp. 963-971.

**Han, F. X.; Zhou, F.; Yang, X. L.; Zhao, J.; Zhao, Y. et al.** (2015): Facile preparation of plga microspheres with diverse internal structures by modified double-emulsion method for controlled release. *Polymer Engineering and Science*, vol. 55, pp. 896-906.

**Heyligers, J. M. M.; Verhagen, H. J. M.; Rotmans, J. I.; Weeterings, C.; de Groot, P. G. et al.** (2006): Heparin immobilization reduces thrombogenicity of small-caliber expanded polytetrafluoroethylene grafts. *Journal of Vascular Surgery*, vol. 43, pp. 587-591.

**Hoshi, R. A.; Van Lith, R.; Jen, M. C.; Allen, J. B.; Lapidus, K. A. et al.** (2013): The blood and vascular cell compatibility of heparin-modified ePTFE vascular grafts. *Biomaterials*, vol. 34, pp. 30-41.

**Hwang, Y. K.; Jeong, U.; Cho, E. C.** (2008): Production of uniform-sized polymer core-shell microcapsules by coaxial electrospraying. *Langmuir*, vol. 24, pp. 2446-2451.

**Lamprecht, A.; Ubrich, N.; Maincent, P.** (2007): Oral low molecular weight heparin delivery by microparticles from complex coacervation. *European Journal of Pharmaceutics and Biopharmaceutics*, vol. 67, pp. 632-638.

**Lee, J. S.; Bae, J. W.; Joung, Y. K.; Lee, S. J.; Dong, K. H. et al.** (2008): Controlled dual release of basic fibroblast growth factor and indomethacin from heparin-conjugated polymeric micelle. *International Journal of Pharmaceutics*, vol. 346, pp. 57-63.

**Li, C. J.; Wang, F. J.; Ge, P.; Mao, Y.; Wang, L. et al.** (2017): Anti-acute thrombogenic surface using coaxial electrospraying coating for vascular graft application. *Materials Letters*, vol. 205, pp. 15-19.

**Li, G. C.; Xie, B.; Pan, C. J.; Yang, P.; Ding, H. et al.** (2014): Facile conjugation of heparin onto titanium surfaces via dopamine inspired coatings for improving blood compatibility. *Journal of Wuhan University of Technology-Materials Science Edition*, vol. 29, pp. 832-840.

**Maitz, M. F.; Zitzmann, J.; Hanke, J.; Renneberg, C.; Tsurkan, M. V. et al.** (2017): Adaptive release of heparin from anticoagulant hydrogels triggered by different blood coagulation factors. *Biomaterials*, vol. 135, pp. 53-61.

**Mei, L.; Liu, Y. Y.; Zhang, H. J.; Zhang, Z.; Gao, H. et al.** (2016): Antitumor and antimetastasis activities of heparin-based micelle served as both carrier and drug. *ACS Applied Materials & Interfaces*, vol. 8, pp. 9577-9589.

**Mouftah, S.; Abdel-Mottaleb, M. M. A.; Lamprecht, A.** (2016): Buccal delivery of low molecular weight heparin by cationic polymethacrylate nanoparticles. *International Journal of Pharmaceutics*, vol. 515, pp. 565-574.

**Murugesan, S.; Xie, J.; Linhardt, R. J.** (2008): Immobilization of heparin: Approaches and applications. *Current Topics in Medicinal Chemistry*, vol. 8, pp. 80-100.

**Qi, W.; Sun, M.; Jing, Z. H.** (2012): Fabrication of chitosan microcapsules via layer-by-layer assembly for loading and *in vitro* release of heparin. *Supramolecular Chemistry*, vol. 24, pp. 350-354.

**Rasekh, M.; Young, C.; Roldo, M.; Lancien, F.; Mével, J. C. L. et al.** (2015): Hollow-layered nanoparticles for therapeutic delivery of peptide prepared using electrospraying. *Journal of Materials Science-Materials in Medicine*, vol. 26, pp. 256-267.

**Tong, F. Y.; Chen, X. Q.; Chen, L. B.; Zhu, P.; Luan, J. et al.** (2013): Preparation, blood compatibility and anticoagulant effect of heparin-loaded polyurethane microspheres. *Journal of Materials Chemistry B*, vol. 1, pp. 447-453.

**Tsung, M.; Burgess, D. J.** (1997): Preparation and stabilization of heparin/gelatin complex coacervate microcapsules. *Journal of Pharmaceutical Sciences*, vol. 86, pp. 603-607.

**Wang, Y.; Wei, Y.; Zhang, X. H.; Xu, M. M.; Liu, F. et al.** (2015): PLGA/PDLLA core-shell submicron spheres sequential release system: Preparation, characterization and promotion of bone regeneration *in vitro* and *in vivo*. *Chemical Engineering Journal*, vol. 273, pp. 490-501.

**Yang, Z. L.; Wang, J.; Luo, R. F.; Maitz, M. F.; Jing, F. J. et al.** (2010): The covalent immobilization of heparin to pulsed-plasma polymeric allylamine films on 316L stainless steel and the resulting effects on hemocompatibility. *Biomaterials*, vol. 31, pp. 2072-2083.

**Zamani, M.; Prabhakaran, M. P.; Thian, E. S. et al.** (2014): Protein encapsulated core-shell structured particles prepared by coaxial electrospraying: Investigation on material and processing variables. *International Journal of Pharmaceutics*, vol. 473, pp. 134-143.

**Zhao, Y.; Lord, M. S.; Stenzel, M. H.** (2013): A polyion complex micelle with heparin for growth factor delivery and uptake into cells. *Journal of Materials Chemistry B*, vol. 1, pp. 1635-1643.